

Identification and characterization of low-mass stars and brown dwarfs using Virtual Observatory tools.

Miriam Aberasturi^{1,2}, Enrique Solano^{1,2}, and Eduardo Martín³

¹ Departamento de Astrofísica. Centro de Astrobiología. P.O.Box 78. 28691. Villanueva de la Cañada, Madrid, Spain.

² Spanish Virtual Observatory.

³ Departamento de Astrofísica. Centro de Astrobiología. Carretera de Ajalvir km 4, 28550 Torrejón de Ardoz, Madrid, Spain.

Abstract

Low-mass stars and brown dwarfs (with spectral types M, L, T and Y) are the most common objects in the Milky Way. A complete census of these objects is necessary to understand the theories about their complex structure and formation processes. In order to increase the number of known objects in the Solar neighborhood ($d < 30$ pc), we have made use of the Virtual Observatory which allows an efficient handling of the huge amount of information available in astronomical databases. We also used the WFC3 installed in the Hubble Space Telescope to look for T5+ dwarfs binaries.

1 Introduction

The low mass stars ($M < 0.6 M_{\odot}$) and brown dwarfs (BDs, $M < 0.07 M_{\odot}$) are the most common and least luminous star-like objects in the Milky Way ([15]). Thousands of these objects, including some of the nearest neighbors to the Sun ([21]; [22]), have been discovered over the past two decades in wide-field optical and infrared imaging surveys such as 2MASS, SDSS, DENIS, UKIDSS, CHFTLS, PansSTARRS and WISE. These findings led to the inclusion of three new spectral types in the spectral classification system: The L, T and Y dwarfs ([13], [5], [8]), with atmospheres governed by molecular gases and condensate chemistry. This sequence represents the path that brown dwarfs (objects with fully convective interiors and that cannot sustain core hydrogen fusion ([18], [19])) follow as they cool down. M-type stars, for their part, have also become of particular interest in recent years for exoplanet surveys. Their low masses and small radii lead to greater sensitivity to discovery of orbiting low mass planets via the radial velocity and transit techniques.

Different theories have been proposed to understand how the low-mass stars and brown dwarfs form: turbulent core fragmentation (e.g., [11]); disk fragmentation (e.g., [16], [17]); dy-

namical interaction and ejection of pre-stellar cores (e.g., [27]); photo-erosion of pre-stellar cores in massive star forming regions ([32]); and instabilities in massive circumstellar disks (e.g., [30]). Observational efforts to complete the census of these objects along with multiplicity studies in star-forming regions and field, would provide us information about which of these mechanisms is dominant.

In order to shed light to these questions, we have made use of the Virtual Observatory (VO¹) to find nearby low-mass stars and brown dwarfs (Section 2, Section 3) and of the Wide Field Camera 3 (WFC3) onboard the Hubble Space Telescope (HST) to find new T5+ binary systems Section 4.

2 WISE/2MASS-SDSS brown dwarfs candidates using Virtual Observatory tools.

In [1] we used VO tools to perform a cross-match of the WISE Preliminary Release, the 2MASS Point Source and the SDSS Data Release 7 catalogues over the whole area of sky that they have in common ($\sim 4000 \text{ deg}^2$). We imposed photometric and proper motion criteria to obtain a list of BD candidates. We have identified 31 BD candidates, 25 of which have already been reported in the literature. The remaining six candidates have been classified as four L- and two T-type objects (see Fig. 1). The high rate of recovery of known BDs ($\sim 90\%$ of the T dwarfs catalogued in 2MASS) demonstrates the validity of our strategy to identify them with VO tools. We estimated the effective temperatures for each candidate based on their spectral energy distribution using VOSA². Spectral types were then estimated following the effective temperature-spectral type relationship given in [14]. Distances, calculated from the absolute magnitude-spectral type relation given in [9] and [6], place three of our candidates at $\sim 20 \text{ pc}$ from the Sun. These candidates, WISE J0821+1443, WISE J0838+1511 and WISE J0920+4538 have been spectroscopically confirmed as brown dwarfs with spectral types L or T. In particular, WISE J0838+1511 have been confirmed by [26] as the first T-dwarf triple system while WISE J0920+4538 is a binary system in the interesting L/T transition region ([23]).

3 Search for bright nearby M dwarfs with Virtual Observatory tools.

In [2], we used Virtual Observatory tools to perform a cross-match of the Carlsberg Meridian 14 (CMC14) and the 2MASS Point Source catalogues to select candidate nearby bright M dwarfs distributed over $\sim 25,000 \text{ deg}^2$. We imposed photometric criteria to obtain a list of M dwarfs candidates (see Fig. 2). In the publication, we present low-resolution optical spectra for 27 candidates that were observed with the Intermediate Dispersion Spectrograph at the 2.5 m Isaac Newton Telescope ($\mathcal{R} \approx 1600$). We derived spectral types from a new spectral

¹<http://www.ivoa.net>

²<http://svo2.cab.inta-csic.es/theory/vosa/>

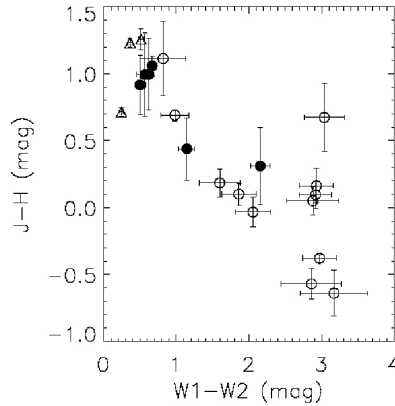


Figure 1: Colour-colour diagram of our six candidates (black full circles) compared with a sample of known L and T dwarfs (triangles and empty circles, respectively) observed with WISE at time of our work ([24]; [29]; [6])

index, \mathfrak{R} , which measures the ratio of fluxes at $7485\text{--}7015\text{\AA}$ and $7120\text{--}7150\text{\AA}$ and used VOSA to derive T_{eff} and $\log g$ for each candidate. The resulting 27 targets were M dwarfs brighter than $J = 10.5$ mag, 16 of which were completely new in the Northern hemisphere and 7 of which were located at less than 15 pc. For all of them, we also measured $H\alpha$ and Na I pseudo-equivalent widths, determined photometric distances, and identified the most active stars. The targets with the weakest sodium absorption, namely J0422+2439 (with X-ray and strong $H\alpha$ emissions), J0435+2523, and J0439+2333, are new members in the young Taurus-Auriga star-forming region based on proper motion, spatial distribution, and location in the color-magnitude diagram, which reopens the discussion on the deficit of M2–4 stars in Taurus (see Fig. 3, e.g. [28]).

4 Constraints on the binary properties of mid to late T dwarfs from Hubble Space Telescope WFC3 observations.

In [3] we used HST/WFC3 observations of a sample of 26 nearby (≤ 20 pc) mid- to late-T dwarfs to search for cooler companions and measure the multiplicity statistics of brown dwarfs. The tightly-separated companions were searched for using a double-PSF fitting algorithm. We also compared our detection limits based on simulations to other prior T5+ brown dwarf binary programs. No new wide or tight companions were identified, which is consistent with the number of known T5+ binary systems and the resolution limit of WFC3. We use our results to add new constraints to the binary fraction of T-type brown dwarfs. Modeling selection effects and adopting previously derived separation and mass ratio distributions, we find an upper limit total binary fraction of $<16\%$ and $<25\%$ assuming power law and flat mass ratio distributions respectively, which are consistent with previous results (see Fig. 4).

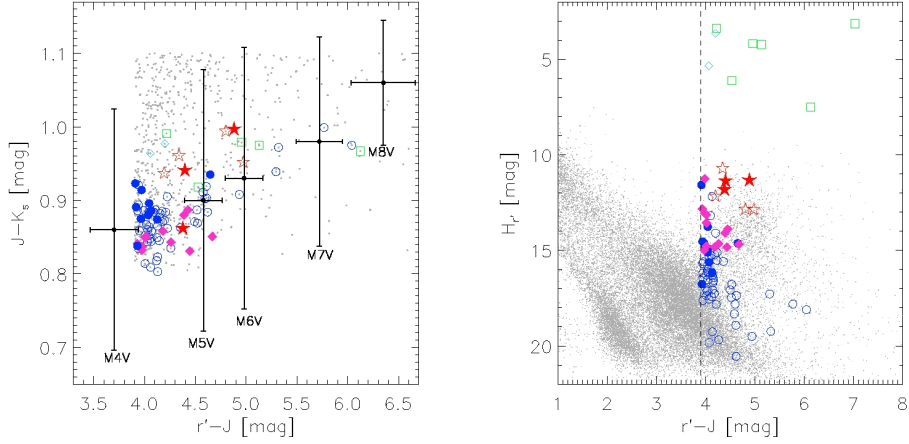


Figure 2: *Left panel:* $J - K_s$ vs. $r' - J$ color-color diagram. Small gray solid points represent the full cross-matched sources. New field M dwarfs are drawn with (magenta) rhombs, previously known field M dwarfs with (blue) circles, members in Taurus-Auriga with (red) stars, M giants with (green) squares, and reddened Cygnus OB2 massive stars with (cyan) rhombs. Black error bars represent the average colors of typical dwarfs of spectral types M4 V to M8 V ([31]). *Right panel:* same as left panel but the tiny gray points represent stars in [20] with CMC14 counterpart. The vertical dashed line at $r' - J = 3.9$ mag indicates our color cut.

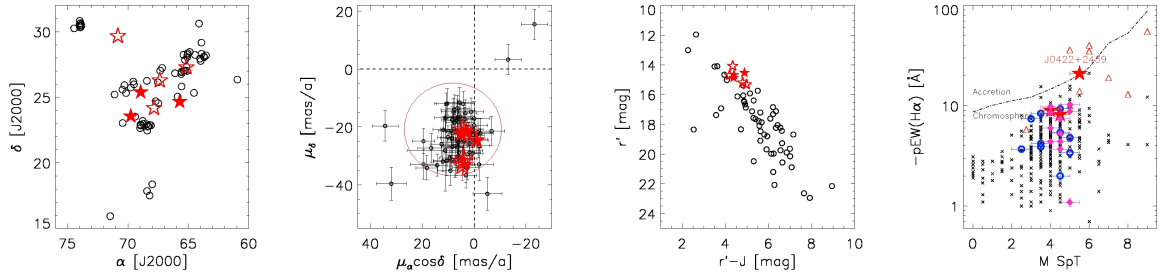


Figure 3: *From left to right:* 1) Spatial distribution of candidate members in the Taurus-Auriga star-forming region. (Red) filled stars are our three new candidates with IDS/INT spectroscopy, (red) open stars are the four known Taurus-Auriga T Tauri stars identified in the 2MASS-CMC14 cross-match, and (gray) open circles are Taurus-Auriga confirmed members; 2) proper-motion diagram. The ellipse indicates the average values and standard deviations of proper motions in Taurus-Auriga from [7], 3) r' vs. $r' - J$ color-magnitude diagram; 4) pseudo-equivalent widths of H α as a function of spectral type. The accretion-chromosphere boundary given in [4] is also drawn. Small (black) crosses are field M dwarfs from [10], (magenta and blue) filled circles are the 24 (new and known) field stars investigated in [2].

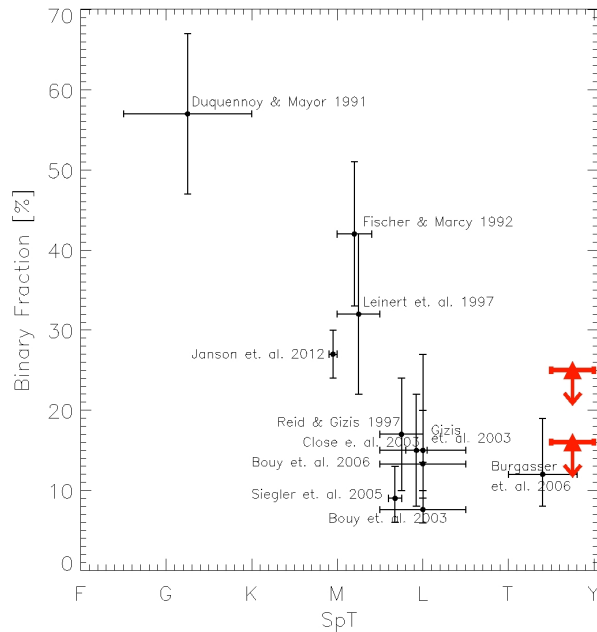


Figure 4: Binary frequency as a function of the spectral type in the field and in clusters. The upper limits determined in this work are shown with red triangles.

Acknowledgments

Thank you to Enrique Solano, Adam Burgasser, Jose Antonio Caballero, Eduardo Martín, Alcione Mora, Benjamín Montesinos, M. Cruz Gálvez-Ortiz, Reid Neil and Dagny Looper. Financial support was provided by the Spanish Ministerio de Ciencia e Innovación under grants AyA2008-02156, AyA2011-24052, AYA2011-30147-C03-03 and EEBB-I-1205556.

References

- [1] Aberasturi, M., Solano, E., & Martín, E. L. 2011, *A&A*, 534, LL7
- [2] Aberasturi, M., Caballero, J. A., Montesinos, B., et al. 2014, *AJ*, 148, 36
- [3] Aberasturi, M., Burgasser, A. J., Mora, A., et al. 2014, *AJ*, 148, 129
- [4] Barrado y Navascués, D., & Martín, E. L. 2003, *AJ*, 126, 2997
- [5] Burgasser, A. J., Geballe, T. R., Leggett, S. K., Kirkpatrick, J. D., & Golimowski, D. A. 2006, *ApJ*, 637, 1067
- [6] Burgasser, A. J., Cushing, M. C., Kirkpatrick, J. D., et al. 2011, *ApJ*, 735, 116
- [7] Bertout, C., & Genova, F. 2006, *A&A*, 460, 499
- [8] Cushing, M. C., Kirkpatrick, J. D., Gelino, C. R., et al. 2011, *ApJ*, 743, 50

- [9] Cruz, K. L., Reid, I. N., Liebert, J., Kirkpatrick, J. D., & Lowrance, P. J. 2003, *AJ*, 126, 2421
- [10] Gershberg, R. E., Katsova, M. M., Lovkaya, M. N., Terebizh, A. V., & Shakhovskaya, N. I. 1999, *A&A*, 139, 555
- [11] Goodwin, S. P., & Whitworth, A. P. 2004, *A&A*, 413, 929
- [12] Hubeny, I., & Burrows, A. 2007, *ApJ*, 669, 1248
- [13] Kirkpatrick, J. D., Reid, I. N., Liebert, J., et al. 1999, *ApJ*, 519, 802
- [14] Kirkpatrick, J. D. 2005, *A&A*, 43, 195
- [15] Kirkpatrick, J. D., Gelino, C. R., Cushing, M. C., et al. 2012, *ApJ*, 753, 156
- [16] Kratter, K. M., Matzner, C. D., & Krumholz, M. R. 2008, *ApJ*, 681, 375
- [17] Kratter, K. M., Murray-Clay, R. A., & Youdin, A. N. 2010, *ApJ*, 710, 1375
- [18] Kumar, S. S. 1962, *AJ*, 67, 579
- [19] Kumar, S. S. 1963, *ApJ*, 137, 1121
- [20] Lépine, S., & Shara, M. M. 2005, *AJ*, 129, 1483
- [21] Luhman, K. L. 2013, *ApJ*, 767, LL1
- [22] Luhman, K. L. 2014, *ApJ*, 786, LL18
- [23] Mace, G. N., Kirkpatrick, J. D., Cushing, M. C., et al. 2013, *ApJ*, 205, 6
- [24] Mainzer, A., Cushing, M. C., Skrutskie, M., et al. 2011, *ApJ*, 726, 30
- [25] Morley, C. V., Fortney, J. J., Marley, M. S., et al. 2012, *ApJ*, 756, 172
- [26] Radigan, J., Jayawardhana, R., Lafrenière, D., et al. 2013, *ApJ*, 778, 36
- [27] Reipurth, B., & Clarke, C. 2001, *AJ*, 122, 432
- [28] Scelsi, L., Maggio, A., Micela, G., et al. 2007, *A&A*, 468, 405
- [29] Scholz, R.-D., Bihain, G., Schnurr, O., & Storm, J. 2011, *A&A*, 532, LL5
- [30] Stamatellos, D., & Whitworth, A. P. 2009, *MNRAS*, 392, 413
- [31] West, A. A., Hawley, S. L., Bochanski, J. J., et al. 2008, *AJ*, 135, 785
- [32] Whitworth, A. P., & Zinnecker, H. 2004, *A&A*, 427, 299